Draft version April 26, 2019
Typeset using LaTeX **modern** style in AASTeX62

A Two Percent Measurement

Will M. Farr,[1,2] Maya Fishbach,[3] Jiani Ye,[1] and Daniel E. Holz[4]

[1] *Department of Physics and Astronomy, Stony Brook University, Stony Brook NY 11794, USA*
[2] *Center for Computational Astronomy, Flatiron Institute, 162 5th Ave., New York NY 10010, USA*
[3] *Department of Astronomy and Astrophysics, University of Chicago, Chicago IL 60637, USA*
[4] *Enrico Fermi Institute, Department of Physics, Department of Astronomy and Astrophysics, and Kavli Institute for Cosmological Physics, University of Chicago, Chicago IL 60637, USA*

ABSTRACT

Joint measurements of distance and redshift can be used to constrain the expansion history of the universe and the associated cosmological parameters CITE. Merging binary black hole (BBH) systems are standard sirens (Schutz 1986; Holz & Hughes 2005)—their gravitational waveform provides direct information about the luminosity distance to the source. Because gravity is scale-free, there is a perfect degeneracy between the source mass and redshift in the waveform; some non-gravitational information is necessary to break the degenracy and determine the redshift of the source (Schutz 1986; Chernoff & Finn 1993; Finn 1996; Wang & Turner 1997; Holz & Hughes 2005; Dalal et al. 2006; Taylor et al. 2012; Messenger & Read 2012; Abbott et al. 2017). Here we suggest that the pair instability supernova (PISN) (Heger & Woosley 2002; Belczynski et al. 2016; Woosley 2017; Spera & Mapelli 2017) process, thought to be the source of the observed upper-limit on the black hole (BH) mass in merging BBH systems at $\sim 45\,M_\odot$ (The LIGO Scientific Collaboration et al. 2018a), provides such information and permits a measurement of the redshift-luminosity-distance relation using a population of BBH inspirals. With realistic assumptions about the merger rate (The LIGO Scientific Collaboration et al. 2018b), a mass distribution incorporating a sharp PISN cutoff (The LIGO Scientific Collaboration et al. 2018a), and measurement uncertainty (Vitale et al. 2017) for BBH inspirals in the Advanced LIGO and Virgo detectors at design sensitivity CITE, we simulate five years of BBH detections. We show that after one year of operation at design sensitivity (put date here) the BBH population can constrain $H(z)$ to 4.1% at a pivot redshift $z \simeq 0.75$.

will.farr@stonybrook.edu
mfishbach@uchicago.edu
jiani.ye@stonybrook.edu
holz@uchicago.edu

After five years (date) the constraint improves to 2.0%. This measurement relies only on general relativity and the presence of a cutoff mass scale that is approximately fixed or calibrated across cosmic time ($\Delta M_{\rm max} \lesssim 1\,M_\odot$); it is independent of any distance ladder or cosmological model. When combined with a percent-level local measurement of the Hubble constant (Chen et al. 2017) and a sub-percent constraint on the physical matter density from CMB measurements (Planck Collaboration et al. 2016) in a wCDM cosmological model, the dark energy equation of state parameter is determined with 9.5% uncertainty. Observations by future "third-generation" gravitational wave (GW) detectors CITE, which can see BBH mergers throughout the universe, would permit sub-percent cosmographical measurements to $z \gtrsim 4$ within one month of observation.

The gravitational wave transient catalog 1 (GWTC1) contains ten binary black hole merger events observed during Advanced LIGO and Advanced VIRGO's first and second observing runs (The LIGO Scientific Collaboration et al. 2018b). Modeling of this population suggests a precipitous drop in the merger rate for primary black hole masses larger than $\sim 45\,M_\odot$ (Fishbach & Holz 2017; The LIGO Scientific Collaboration et al. 2018b). A possible explanation for this drop is the PISN process CITE. This process occurs in the cores of massive stars (helium core masses 30–133 $M_\odot$ (Woosley 2017)) when the core temperature becomes sufficiently high to permit the production of electron-positron pairs; pair production softens the equation of state of the core, leading to a collapse which is halted by nuclear burning (Heger & Woosley 2002). The energy produced can either unbind the star, leaving no BH remnant, or drive a mass-loss pulse that reduces the mass of the star until the PISN is halted, leading to remnant masses $\sim 45\,M_\odot$. Modeling suggests that the upper limit on the remnant mass may vary by less than XX with redshift for $0 \leq z \lesssim 2$ (Belczynski et al. 2016).

Compact object mergers that emit gravitational waves have a universal characteristic peak luminosity $c^5/G \simeq 3.6 \times 10^{59}\,{\rm erg\,s^{-1}}$ that enables direct measurements of the luminosity distance to these sources (Schutz 1986). They are standard sirens (Holz & Hughes 2005). However, the source-frame mass of the merging objects is degenerate with the redshift; the waveform depends only on the redshifted mass in the detector frame, $m_{\rm det} = m_{\rm source}(1+z)$. General relativity predicts the gravitational waveforms of stellar-mass BBH mergers. Using parameterized models of these waveforms (Taracchini et al. 2014; Khan et al. 2016; Bohé et al. 2017; Chatziioannou et al. 2017), it will be possible to measure the detector-frame masses with $\sim 20\%$ uncertainty and luminosity distances (Hogg 1999) with $\sim 50\%$ uncertainty for a source near the detection threshold in Advanced LIGO and Anvanced Virgo at design sensitivity (Vitale et al. 2017) CITE. The uncertainty in these parameters scales inversely with the signal-to-noise ratio of a source (Vitale et al. 2017).

If the BBH merger rate follows the star formation rate (Fishbach et al. 2018; The LIGO Scientific Collaboration et al. 2018a), the primary mass distribution follows a declining power law $m_1^{-\alpha}$ with $\alpha \simeq 0.75$ for $m_1 \lesssim 45\,M_\odot$, the mass ratio distribution is flat, and the three-detector duty cycle is $\sim 50\%$ then Advanced LIGO and Advanced Virgo should detect ~ 1000 BBH mergers per year at design sensitivity over a range of redshifts $0 \leq z \lesssim 1.5$. The typical detected merger will have a redshift $z \sim 0.75$. If we assume that $\sim 1/2$ these detections are informative about the redshifted upper limit on the remnant mass in the detector frame, $m_{\rm max,det} = m_{\rm max,source}\,(1 + z\,(d_L))$, that the combined uncertainty is $1/\sqrt{N}$ smaller than the single-measurement uncertainty, and that most detections are near threshold, then we are dominated by the $\sim 50\%$ distance uncertainty and can achieve an absolute distance-redshift measurement (i.e. constrain the local expansion rate, $H(z)$, for $z \simeq 0.75$) at the $50\%/\sqrt{1000/2} \simeq 2.2\%$ level after one year, and the 1% level after five years of BBH merger observations at design sensitivity.

Detailed calculations support this back-of-the-envelope estimate. We have simulated five years of GW observations with Advanced LIGO and Advanced Virgo at design sensitivity. We use a local merger rate, mass distribution, and rate evolution with redshift that are consistent with current observations (Fishbach & Holz 2017; Fishbach et al. 2018; The LIGO Scientific Collaboration et al. 2018a). Our mass distribution includes a sharp cutoff at $m = 45\,M_\odot$ to model the effects of the PISN process (Belczynski et al. 2016). We use a realistic model of the detectability of sources from this population (Abbott et al. 2016a,b) and for mass and distance estimation uncertainties (Vitale et al. 2017). The properties of the simulated population are described more fully in §A.

We thank Stephen Feeney for providing a sounding board for the methods discussed in this paper. We acknowledge the 2018 April APS Meeting and Barley's Brewing Company in Columbus, OH, USA where this work was originally conceived.

REFERENCES

Abbott, B. P., Abbott, R., Abbott, T. D., et al. 2016a, ApJ, 833, L1, doi: 10.3847/2041-8205/833/1/L1

—. 2016b, The Astrophysical Journal Supplement Series, 227, 14, doi: 10.3847/0067-0049/227/2/14

—. 2017, Nature, 551, 85, doi: 10.1038/nature24471

Aubourg, É., Bailey, S., Bautista, J. E., et al. 2015, PhRvD, 92, 123516, doi: 10.1103/PhysRevD.92.123516

Aylor, K., Joy, M., Knox, L., et al. 2019, ApJ, 874, 4, doi: 10.3847/1538-4357/ab0898

Belczynski, K., Heger, A., Gladysz, W., et al. 2016, A&A, 594, A97, doi: 10.1051/0004-6361/201628980

Bohé, A., Shao, L., Taracchini, A., et al. 2017, PhRvD, 95, 044028, doi: 10.1103/PhysRevD.95.044028

Chatziioannou, K., Klein, A., Yunes, N., & Cornish, N. 2017, PhRvD, 95, 104004, doi: 10.1103/PhysRevD.95.104004

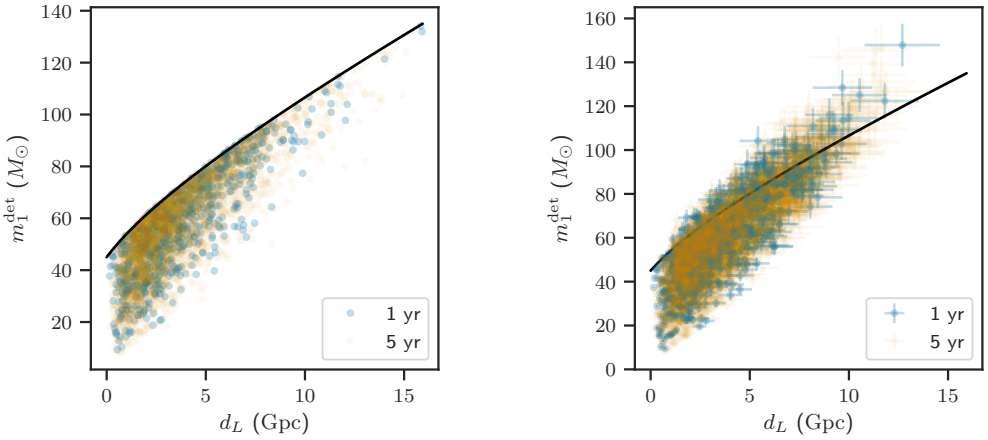

Figure 1. Simulated population of BBH mergers. (Left) The true detector-frame primary BH masses and luminosity distances for the simulated population of BBH mergers used in this work. Blue circles denote one year of Advanced LIGO / Virgo observations, orange circles five years of observations. The black line shows the redshifting of the maximum BH mass corresponding to the cosmology used to generate the events (Planck Collaboration et al. 2016, TT, TE, EE + lowP + lensing + ext). (Right) The inferred detector-frame primary BH masses and luminosity distances using our model for the GW data likelihood for each BBH event. Here again blue corresponds to one year of observations and orange to five years. Dots denote the mean and bars the 1σ width of the likelihood (i.e. a posterior distribution using flat priors on m_1 and d_L). There is a bias in the recovery of the masses and distance that becomes more acute at large distances due to a failure to model the population (which is not flat in m_1 and d_L) and selection effects in these single-event analyses. The black line shows the redshifting of the mass upper limit. The most-distant event biases upward in both mass and distance by several sigma because it represents a single "lucky" noise fluctuation into detectability out of $\sim 2 \times 10^5$ merger events per year within the detector horizon.

Chen, H.-Y., Fishbach, M., & Holz, D. E. 2017, ArXiv e-prints, arXiv:1712.06531. https://arxiv.org/abs/1712.06531

Chernoff, D. F., & Finn, L. S. 1993, ApJ, 411, L5, doi: 10.1086/186898

Cuesta, A. J., Verde, L., Riess, A., & Jimenez, R. 2015, MNRAS, 448, 3463, doi: 10.1093/mnras/stv261

Dalal, N., Holz, D. E., Hughes, S. A., & Jain, B. 2006, PhRvD, 74, 063006, doi: 10.1103/PhysRevD.74.063006

Feeney, S. M., Peiris, H. V., Williamson, A. R., et al. 2019, PhRvL, 122, 061105, doi: 10.1103/PhysRevLett.122.061105

Finn, L. S. 1996, PhRvD, 53, 2878, doi: 10.1103/PhysRevD.53.2878

Fishbach, M., & Holz, D. E. 2017, ApJ, 851, L25, doi: 10.3847/2041-8213/aa9bf6

Fishbach, M., Holz, D. E., & Farr, W. M. 2018, ArXiv e-prints, arXiv:1805.10270. https://arxiv.org/abs/1805.10270

Heger, A., & Woosley, S. E. 2002, ApJ, 567, 532, doi: 10.1086/338487

Hogg, D. W. 1999, ArXiv e-prints, astro. https://arxiv.org/abs/astro-ph/9905116

Holz, D. E., & Hughes, S. A. 2005, ApJ, 629, 15, doi: 10.1086/431341

Khan, S., Husa, S., Hannam, M., et al. 2016, PhRvD, 93, 044007, doi: 10.1103/PhysRevD.93.044007

Messenger, C., & Read, J. 2012, PhRvL, 108, 091101, doi: 10.1103/PhysRevLett.108.091101

Mortlock, D. J., Feeney, S. M., Peiris, H. V., Williamson, A. R., & Nissanke, S. M. 2018, arXiv e-prints, arXiv:1811.11723. https://arxiv.org/abs/1811.11723

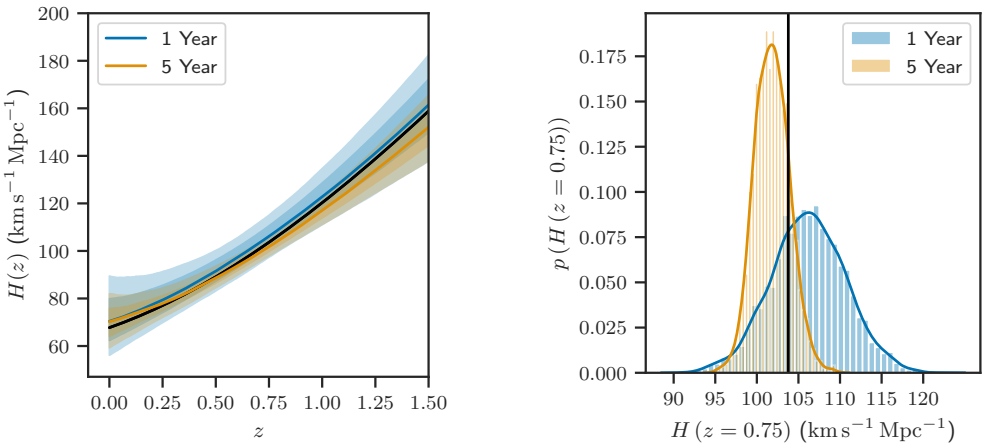

Figure 2. Inferred cosmological expansion history and distance scale. (Left) The local expansion rate, $H(z)$, inferred from an analysis of the one year (blue) and five year (orange) simulated populations using a mass distribution model with a parameterized cutoff mass (see text). The black line gives the cosmology used to generate the simulated population (Planck Collaboration et al. 2016, TT, TE, EE + lowP + lensing + ext). The solid lines give the posterior median $H(z)$ at each redshift; the bands give 1σ (68%) and 2σ (95%) credible intervals. The 1σ fractional uncertainty on $H(z)$ is minimized at $z \simeq 0.75$ for both data sets; after one year it is 4.1% and after five years it is 2.0%. (Right) Posterior distributions over $H\,(z = 0.75)$, corresponding to the redshift where the fractional uncertainty is minimized. The true $H\,(z = 0.75)$ is shown by the black vertical line. The posterior after one year is blue, after five years is orange. This demonstrates an absolute distance measure to $z \simeq 0.75$ at percent-level precision; combining this inference on $H(z)$ with other data sets such as observations of baryon acoustic oscillations (Aubourg et al. 2015) or Type Ia supernovae (Scolnic et al. 2018) can translate this absolute distance measure to other redshifts (Aubourg et al. 2015; Cuesta et al. 2015; Feeney et al. 2019). For example, one can independently calibrate the Type Ia supernova distance scale without a distance ladder (Feeney et al. 2019; Scolnic et al. 2018), or compare the GW-determined distance scale with one derived from the photon-baryon sound horizon (Cuesta et al. 2015; Aylor et al. 2019) in the early universe (Planck Collaboration et al. 2016) or at late times (Aubourg et al. 2015).

Planck Collaboration, Ade, P. A. R., Aghanim, N., et al. 2016, A&A, 594, A13, doi: 10.1051/0004-6361/201525830

Schutz, B. F. 1986, Nature, 323, 310, doi: 10.1038/323310a0

Scolnic, D. M., Jones, D. O., Rest, A., et al. 2018, ApJ, 859, 101, doi: 10.3847/1538-4357/aab9bb

Spera, M., & Mapelli, M. 2017, MNRAS, 470, 4739, doi: 10.1093/mnras/stx1576

Taracchini, A., Buonanno, A., Pan, Y., et al. 2014, PhRvD, 89, 061502, doi: 10.1103/PhysRevD.89.061502

Taylor, S. R., Gair, J. R., & Mandel, I. 2012, PhRvD, 85, 023535, doi: 10.1103/PhysRevD.85.023535

The LIGO Scientific Collaboration, the Virgo Collaboration, Abbott, B. P., et al. 2018a, arXiv e-prints, arXiv:1811.12940. https://arxiv.org/abs/1811.12940

—. 2018b, arXiv e-prints, arXiv:1811.12907. https://arxiv.org/abs/1811.12907

Vitale, S., Lynch, R., Raymond, V., et al. 2017, PhRvD, 95, 064053, doi: 10.1103/PhysRevD.95.064053

Wang, Y., & Turner, E. L. 1997, PhRvD, 56, 724, doi: 10.1103/PhysRevD.56.724

Woosley, S. E. 2017, ApJ, 836, 244, doi: 10.3847/1538-4357/836/2/244

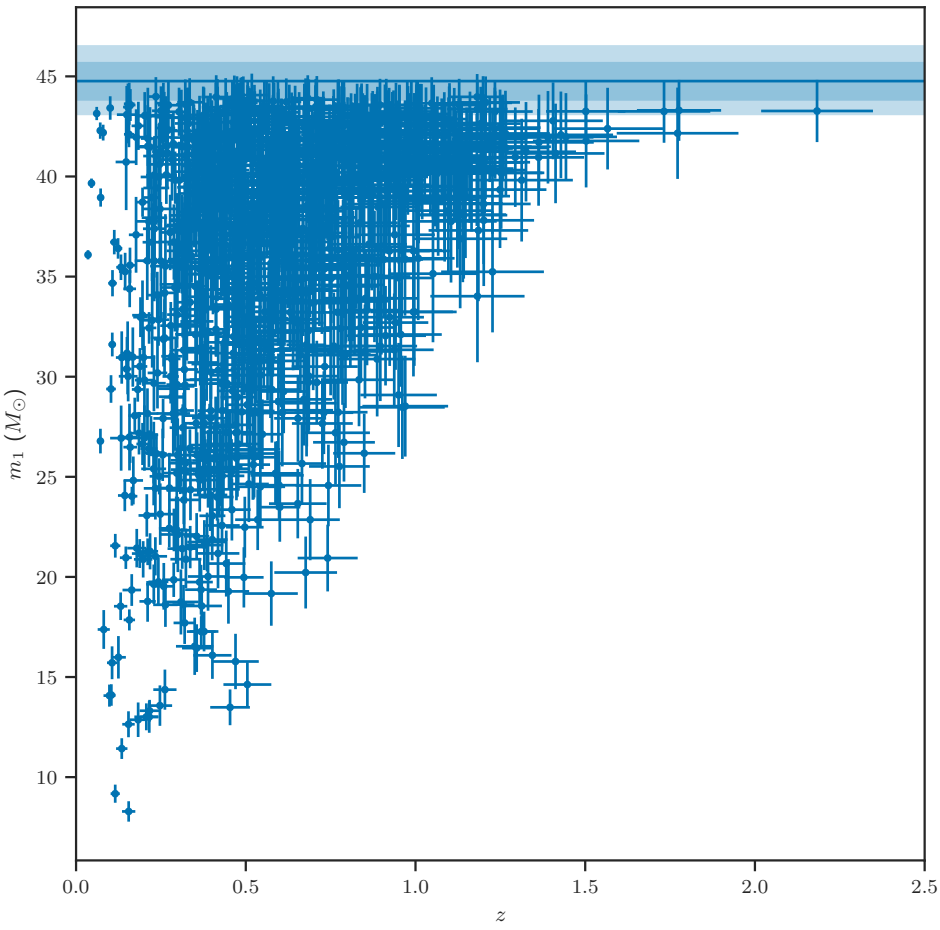

Figure 3. Inferred maximum mass and masses and redshifts for one year of observation. Posterior mean and 1σ (68%) credible ranges for the source-frame primary BH mass and redshift after one year of BBH merger observations. The horizontal line is the posterior median of the maximum black hole mass set by the PISN process; the dark and light bands correspond to the 1σ and 2σ (68% and 95%) credible intervals on the maximum mass. (Compare to Figure 1.) Our model adjusts cosmological parameters, and therefore the correspondence between the measured detector-frame masses and luminosity distances and inferred redshifts and source-frame masses, until it achieves a consistent upper limit on the source-frame BH mass across all redshifts. After one year of synthetic observations we measure $M_{\rm max} = 44.76^{+0.90}_{-0.95}\,M_\odot$ (median and 68% credible interval). After five years (not shown) we measure $M_{\rm max} = 45.14^{+0.46}_{-0.57}\,M_\odot$.

APPENDIX

A. SIMULATED POPULATION

Blah.

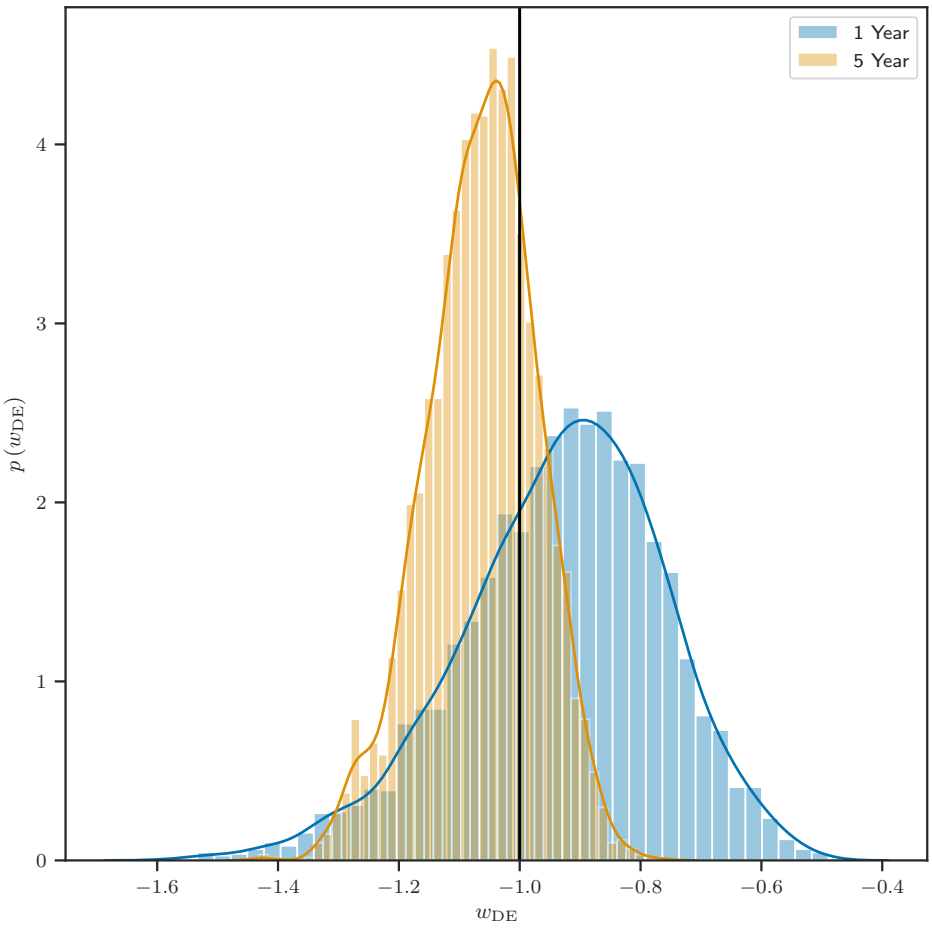

Figure 4. Posterior on the dark energy equation of state parameter after imposing additional cosmological constraints. If we impose a 1% measurement of H_0 (Chen et al. 2017; Mortlock et al. 2018) and the constraints on $\Omega_M h^2$ from existing observations of the cosmic microwave background (Planck Collaboration et al. 2016), we can infer the equation of state parameter $w_{\rm DE} \equiv P_{\rm DE}/\rho_{\rm DE}$ for dark energy in a wCDM cosmological model. (We do not obtain any meaningful constraint on the evolution of $w_{\rm DE}$ with redshift when this parameter is allowed to vary, so we fix it to a constant across all redshifts.) We use $w_{\rm DE} = -1$ to generate our data set; this value is indicated by the black line above. The posterior obtained on $w_{\rm DE}$ after one year of synthetic observations is shown in blue and after five years in orange. We find $w_{\rm DE} = -0.91^{+0.15}_{-0.17}$ after one year (median and 68% credible interval) and $w_{\rm DE} = -1.056^{+0.087}_{-0.102}$ after five years.